Ceramics International 46 (2020) 13989–13996

Contents lists available at ScienceDirect

Ceramics International

journal homepage: www.elsevier.com/locate/ceramint

Influence of long-term thermal aging on the microstructural and tensile properties of all-oxide ceramic matrix composites

Hui Liu[a], Changhao Pei[a], Junjie Yang[a], Zhengmao Yang[b,*]

[a] School of Aerospace Engineering, Tsinghua University, Beijing, China
[b] Institute of Mechanics, Chinese Academy of Sciences, Beijing, China

ARTICLE INFO

Keywords:
Ceramic-matrix composites (CMCs)
Lone-term thermal aging
Microstructure evolution
Mechanical properties

ABSTRACT

The mechanical properties of Nextel™610-reinforced ceramic composites in the on-axis direction after a long-term thermal exposure at 1200°C for 200 h are studied using tensile tests. To clarify the mechanisms underlying the effects of thermal exposure on the macromechanical properties of oxide/oxide ceramic matrix composites, variations in the microstructure and micromechanical properties of these materials (including the fibre grain size and the porosity distribution) are analyzed. Grain coarsening is the most significant feature arising from heat treatment and porosity decreases with increasing heat-treatment time. The dimensions and weight of the specimen also decrease. Given the microstructural changes observed after heat treatment, a model based on mesoscopic-scale approaches is proposed to clarify the influence of thermal exposure on the mechanical properties of the composite, including its stiffness, ultimate failure modes, and strength.

1. Introduction

Ceramic-matrix composites are some of the most promising materials for high-temperature applications owing to their exceptional properties such as their specific stiffness, specific strength, and oxidation resistance in extreme high-temperature and corrosive environments. Although the oxide/oxide ceramic matrix composites exhibit a high oxidation resistance, long-term exposure to a thermal-overloading environment in an aeroengine causes the degradation of their mechanical properties [1–5], with obvious implications for the service performance of ceramic matrix composite components. Therefore, it is important to clarify the effects of thermal-exposure conditions on the mechanical properties of such composites.

Intensive research has been conducted on the evolution of ceramic matrix composite microstructures during thermal exposure. Microstructural variations in different components made from oxide/oxide ceramic matrix composites have been studied. Effects of thermal overloading, with regard to its temperature and duration, on the strength of oxide-fibre bundles were discussed by Schmücker [6,7]. The fine-grained fibre microstructure is not stable at high temperatures and the fibre strength decreases with increasing fibre grain size [7,8]. Vokmann [9] analyzed the evolution of the oxide-fibre microstructure in ceramic matrix composites, and indicated that the matrix composition significantly influences the fibre microstructure after heat treatment. Sintering the matrix accelerates fibre grain coarsening. As the bearing capacity of composites is mainly determined by the fibre properties, the overall performance, especially the composite strength, decreases after thermal exposure. Then, because of the matrix densification induced by sintering, it is clear that the microhardness and microporosity increase and the macroporosity decreases [10].

The effects of heat treatment on static properties such as strength and stiffness have been widely studied [11–13]. Despite extensive studies into the evolution of the microstructure and mechanical properties during thermal exposure, their correlations after heat treatment have not been adequately investigated to date. The underlying mechanism governing the influence of thermal exposure also awaits further investigation. Recently, Yang [14] presented an experimental study on a long-fibre-reinforced oxide/oxide ceramic matrix composite (Ox-CMC), focusing on the thermally induced damage produced after aging at 1200°C for up to 500 h. An analytical model was also proposed, describing the relation between the change in porosity due to thermal aging, damage, and compressive strength.

In the present work, oxide/oxide ceramic matrix composites were heat-treated for 100, 200, and 500 h at 1200°C. The microstructure of different components of the as-received and heat-treated composites were analyzed by several microstructure observation methods. Then, on-axis tensile tests were conducted on the as-received materials and on the heat-treated materials following different heat-treatment durations

* Corresponding author.
E-mail address: zmyang@imech.ac.cn (Z. Yang).

https://doi.org/10.1016/j.ceramint.2020.02.198
Received 6 December 2019; Received in revised form 7 February 2020; Accepted 20 February 2020
Available online 25 February 2020

to study the effects of thermal exposure on the on-axis mechanical properties of the composites. The failure modes of the as-received and heat-treated materials have been discussed. Then, the correlation between the microstructural variations in the fibre and matrix material and the overall mechanical properties (including the stiffness and strength) on the mesoscopic scale have been discussed, based on the observations of microstructure variations and mechanical experimental data.

2. Materials and experimental procedure

2.1. Characterization of the as-received material

The as-received ceramic matrix composite studied in the present work is composed of an uncoated Nextel™610 fibre reinforcement in 8HSW with a woven layer of 0˚/90˚ and a porous matrix containing 85% Al_2O_3 and 15% 3YSZ, which is provided in the form of 2.8-mm-thick plates. The textile structures were impregnated with the paste-like Al_2O_3 slurry using knife blade. Then stack 8 layers together, press and dry at 80˚C-150˚C. After that the sintering process was began at 1100˚C-1300˚C for 5 h. The ultimate continuous service temperature is 1150˚C. The fibre volume content of the composite is approximately 44 vol%. The mechanical properties of the as-processed fibre and material, including the elastic modulus E and ultimate strength σ_u, are listed in Table 1

The original elastic modulus of the matrix is notably close to that of the fibre. However, the strength of the matrix is considerably less than that of the fibre.

2.2. Heat treatment and mechanical experimental procedure

To clarify the effects of heat treatment on the microstructure and mechanical properties of the oxide/oxide ceramic matrix composite, some materials were placed in the high-temperature ambient environment of a muffle furnace (at 1200 ˚C), separately for 100, 200, or 500 h, and cooled in air naturally. A temperature increase rate of 10 ˚C/min, up to the maximum temperature, was chosen to avoid causing additional thermal damage to the material, further details for the heat treatment tests can be found in Ref. [14].

The present work investigated the influence of heat treatment on the changes in the mechanical properties of the ceramic matrix composite by conducting monotonic tensile tests on both as-received and heat-treated materials in the 0˚ direction at ambient temperature based on the ASTM standard C1275. Monotonic loading tests were performed in displacement-control mode with a loading speed of 0.001 mm/s to ensure a quasi-static loading process. All the tests were conducted by MTS809. To determine the mechanical properties of the ceramic matrix composite after heat treatment, several dog-bone-shaped specimens with a gauge length of 35 mm (as displayed in Fig. 1) were machined using a water-jet, and strain rosettes were used to determine the strain states in the gauge section of the specimens. As the stiffness and strength of the composite is mainly dependent on the elastic modulus and strength of matrix and fiber which are related to the microstructure of these components directly, some essential characteristics of matrix and fiber are studied including the porosity of the material and grain size of fibre before and after heat treatment. Mercury intrusion is a widely adopted method for measuring porosity and the size distribution of open holes in porous materials. We measured the porosity using a Micromeritics Autopore IV 9510 porosimeter at room temperature in a vacuum. Then the grain size of fibre are observed by SEM.

Table 1
Mechanical properties of the as-processed fibre and matrix material [14–17].

material composition	E (GPa)	σ_u(MPa)
Fibre (99% Al_2O_3)	373	2930
Matrix (85% Al_2O_3 15% 3YSZ)	210	45

3. Microstructure variations and experimental results

3.1. Microstructure variations of the material after heat treatment

To investigate the effects of thermal exposure on the oxide/oxide ceramic matrix microstructure, SEM observations were conducted on the cutting surface of the as-received and heat-treated materials after 500 h of thermal exposure. The obtained SEM images are shown in Fig. 2.

The matrix region of the as-received material displays many voids and cracks resulting from matrix shrinkage, induced by thermal stress during the preparation of the composite. The fibres are dense and the matrix contains voids and numerous microcracks. Then, because there is no fibre coating at the interface, a microscopic gap is formed between the fibre and the matrix.

As the mechanical properties of the oxide/oxide ceramic matrix composite are directly related to the internal microstructure, it is essential to investigate the effects of thermal exposure on the material microstructures. The present work therefore performed microstructural measurements, in particular for the porosity, morphology, and grain size of fibres.

The measurement results for the as-received and heat-treated materials (after 100, 200, and 500 h of thermal exposure) are characterized in Ref. [14]. The overall porosity of these materials can be obtained from the intersections of the corresponding curve with the y-axis, as listed in Table 2.

The measurements indicate an overall decrease in the porosity of the oxide/oxide ceramic matrix composite with increasing heat-treatment time, which may be induced by matrix sintering. For a heat-treatment duration less than 100 h, the overall composite porosity decreases rapidly with increasing heat-treatment time. Then, between 100 and 200 h, the overall porosity also decreases significantly with increasing thermal-exposure duration, albeit significantly more slowly. Heat treatment beyond 200 h shows no clear reduction in the overall porosity.

Long-term exposure also affects the oxide-fibre microstructure significantly, with noteworthy consequences for the mechanical properties, especially the strength dominated by fibres. The present study therefore investigates the fibre microstructures in the original and heat-treated materials. The thermal corrosion method was adopted. SEM images of the fibre microstructures are displayed in Fig. 3, showing the grain-size distributions for (a) the original and (b) the heat-treated materials (after 500 h of thermal exposure).

The areas bounded by yellow lines represent grain crystals in the material.

A comparison of Fig. 3(a) and (b) reveals some microstructural variations. The fibres of the as-received material contain only single-phase $\alpha-$ alumina. After heat treatment, some highly dispersed crystallites are created and the average grain size increases relative to the original material. In other words, a significant coarsening of α-alumina is induced by thermal exposure, causing significant changes in the mechanical properties.

The first part of the present article characterized the microstructure variations of the components of the composite, namely the matrix and fibres. The next section discusses the relationship between variations in the overall mechanical properties, namely the stiffness, failure modes, and strength.

3.2. Mechanical properties of the as-received and heat-treated materials

Stress-strain curves, obtained from uniaxial tension experiments in the on-axis direction of specimens subjected to different exposure durations, are plotted in Fig. 4.

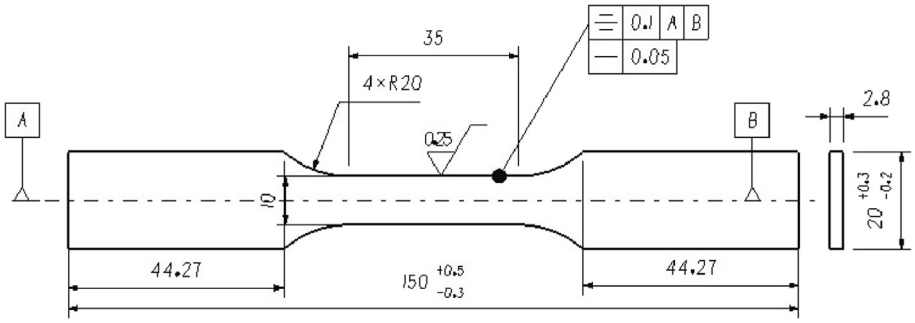

Fig. 1. Schematic specimen cross section.

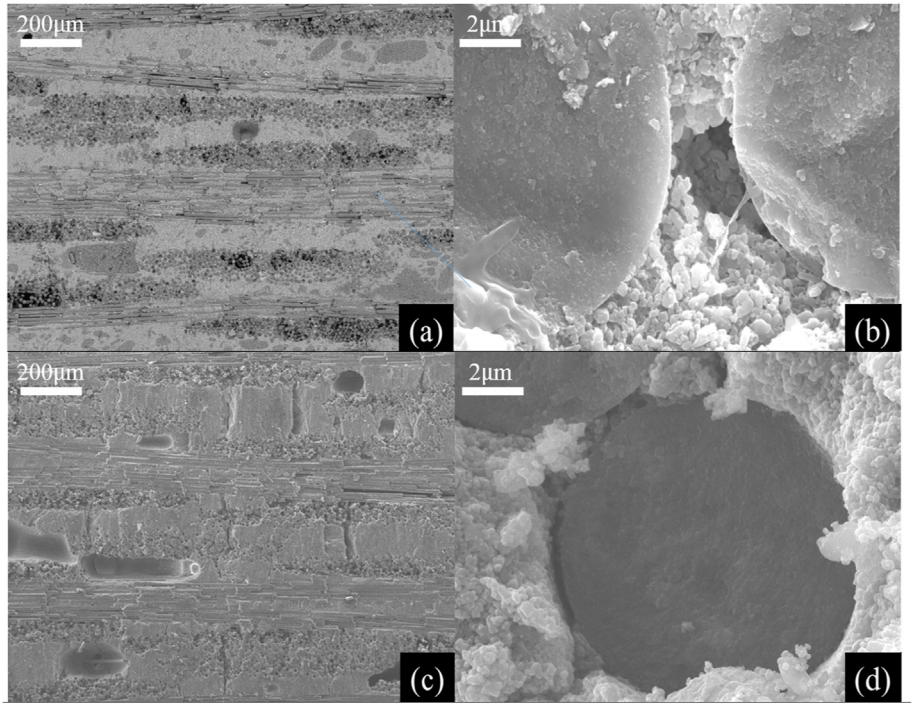

Fig. 2. SEM images of cut surfaces for (a,b) the as-received material and (c,d) the material after 500 h of heat treatment. The most obvious microstructural changes are the appearance of fibre bridging in the interface and the direct fibre-matrix connection after heat treatment.

Table 2
Porosity of the material for different thermal-exposure durations.

	as-received	100 h	200 h	500 h
Porosity	27.6 (%)	24.9 (%)	21.8 (%)	21.6 (%)

The monotonic tensile experimental data indicate no clear nonlinear behaviour in the stress-strain curve for either the as-received or heat-treated materials. The elastic modulus after heat treatment is almost identical to that of the original material. Then, the failure stress and failure strain decrease significantly after thermal exposure, indicating that heat treatment increases the brittleness of the material. According to Fig. 4, the residual strength following heat treatment is directly related to the thermal-exposure duration. The failure stresses after

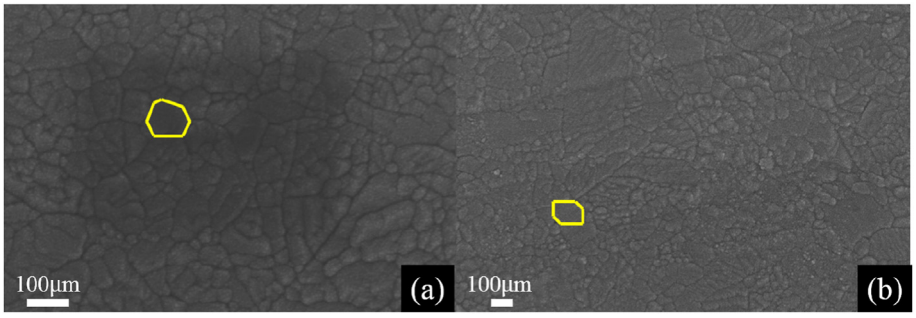

Fig. 3. Fibre microstructures in (a) the as-received and (b) the heat-treated materials after 500 h of thermal exposure.

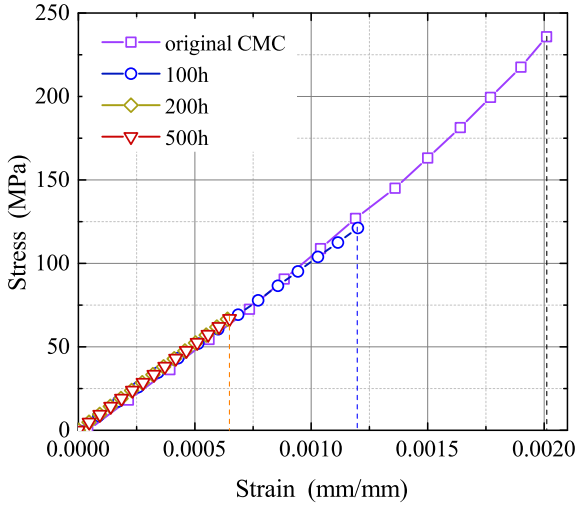

Fig. 4. Stress-strain curves for the as-received and heat-treated materials in the 0° direction.

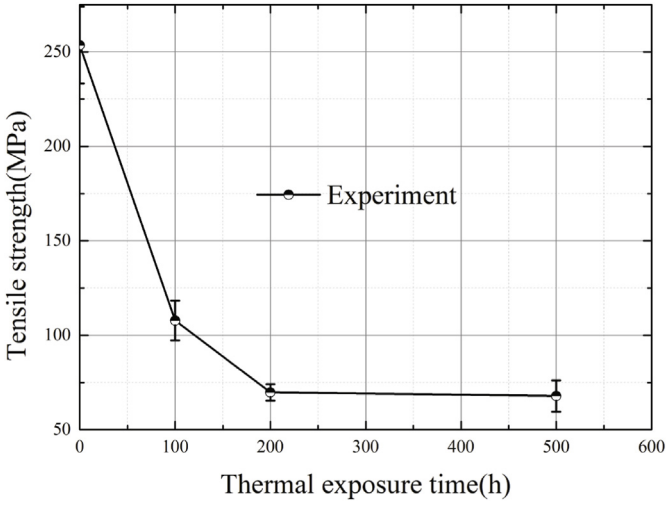

Fig. 5. Residual strength versus thermal-exposure duration.

different heat-treatment durations are displayed in Fig. 5.

From Fig. 5, the trend followed by the failure stress is exactly similar to that of the fibre grain size and the overall porosity of the composite. Considering the relationship between the microstructure and mechanical properties of the composite, this phenomenon implies that the oxide/oxide ceramic matrix composite microstructure becomes stable gradually with increasing heat-treatment time, consistent with observations and measurements of the microstructure of the constituting fibre and matrix. The effects of variations in the fibre and matrix on the overall mechanical properties of the composite are discussed in the following section.

4. Effects of thermal aging on the mechanical properties of the ceramic matrix composites

As a result of the changes in the microstructure and micromechanical properties induced by long-term thermal exposure, the mechanical behaviour of the heat-treated composites subjected to stress differ from the as-received material. This has significant implications for the service performance of composite components. Thus, it is important to study the change regularities of microstructure and micromechanical properties and their effects on the mechanical behaviour. As microstructural changes have already been discussed 4 above, their effects on the mechanical behaviour, including elastic properties and ultimate failure, are analyzed below.

4.1. Effects of thermal exposure on the stiffness of the ceramic matrix composites

The composite stiffness depends on the fibre and matrix elastic moduli, implying that changes in the fibres and matrix during thermal exposure can significantly influence the overall stiffness of the material. The influence rule is discussed in the following section.

The overall stiffness of a unidirectional fibre-reinforced composite can be approximated as

$$E_c = E_f V_f + E_m V_m \tag{1}$$

In a woven composite, considering the distinction between longitudinal and transverse fibre bundles, approximately half of the fibres bear the uniaxial tensile loading in the warp direction. Thus, Eq. (1) can be rewritten as

$$E_c = \omega E_f + E_m(1 - \omega) \tag{2}$$

where E is the elastic modulus; the subscripts c, f, and m denote the composite, fibre, and matrix, respectively; and ω is the effective fibre volume fraction (which represents effects of the volume fraction of longitudinal fibres). Based on experimental measurements of the original elastic modulus, ω is considered to be 0.09.

According to Ref. [18], the matrix elastic modulus depends directly on the porosity:

$$\frac{E_m}{E_m^0} = \left(\frac{1-\rho}{1-\rho_0}\right)^n \tag{3}$$

where E_m^0 and E_m denote the initial and current elastic moduli of the matrix.

Thermal exposure induces some microstructural changes in the fibre and matrix, which in turn induce variations in the mechanical properties. According to Volkmann [10], the fibre elastic modulus changes negligibly. Thus, the matrix stiffness can be considered to play an important role in the evolution of the overall stiffness of an oxide/oxide ceramic matrix composite. Substituting Eq. (3) into Eq. (2), the overall elastic modulus of a woven oxide/oxide ceramic matrix composite becomes

$$E_c = \omega E_f + (1 - \omega)E_m^0\left(\frac{1-\rho}{1-\rho_0}\right)^n \tag{4}$$

Eq. (4) relates the variations in the composite elastic modulus and to those in the porosity. The result is plotted in Fig. 6, with the horizontal and vertical coordinates being normalized by the porosity of the as-

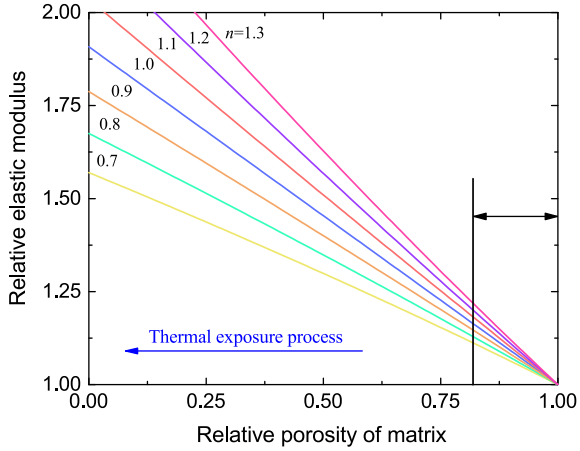

Fig. 6. Relationship between the elastic modulus and the relative porosity of the material for different values of n.

received matrix and the original elastic modulus.

The effects of using different values of n in Eq. (3) are shown in Fig. 6. Seven values of n were chosen in the range 0.7–1.3, which is considered to apply to an oxide/oxide ceramic matrix composite (18). Notably, there is an approximately linear relationship between the relative elastic modulus of the composite and the relative porosity of the matrix material. Based on the relationship between thermal-exposure duration and the matrix porosity, the variations of the elastic modulus can then be determined. According to the relationship proposed in Ref. [14], the variation range of the porosity shown in Fig. 6 is small. For a sufficiently long thermal exposure, the material porosity shows almost no decrease, and therefore the overall stiffness of the material in the on-axis direction changes insignificantly.

4.2. Effects of thermal exposure on the ultimate failure and strength of the ceramic matrix composites

The above analysis suggests that the thermal-exposure duration has only a very small effect on the overall elastic modulus of the composite, consistent with the experimental result that the on-axis elastic modulus of the material varies insignificantly with the thermal-exposure duration.

To investigate the failure mechanisms of the as-received and heat-treated materials, their fracture surfaces were observed by SEM, as shown in Fig. 7.

The fracture surfaces of the as-received and heat-treated materials are relatively smooth, indicating that brittle fracture plays a dominant role in the failure process in these materials. However, the fibre pull-out phenomenon can be observed in Fig. 7(a). Subsequent to heat treatment, it almost disappears completely, and only fibre breakage is observed in Fig. 7(b). These changes in the fracture surface imply that sliding at the interface is suppressed, or even disappears, because of fibre bridging during heat treatment, as observed in Fig. 2. They also imply that the failure mode of the composite changes essentially as a result of variations in the fibre, matrix, and interface of the material.

According to theory [19–21], when a mechanical load is applied to a porous-matrix ceramic composite without a fibre coating, matrix cracks form and subsequently propagate as the external load increases. As a matrix crack extends to the fibre-matrix interface, it becomes deflected along the interface or penetrates into the adjacent fibre, depending on the intrinsic properties of the composite components. The relationship between the mode of propagation of matrix cracks and the mechanical properties of the material is exhibited in Fig. 8.

The relationship shown in Fig. 8 involves two control parameters to analyze crack propagation at the interface: the elastic mismatch parameter $(E_f\text{-}E_m)/(E_f + E_m)$ and the transition toughness ratio Γ_i/Γ_f (see Fig. 9). E_f and E_m denote the fibre longitudinal stiffness and the matrix elastic modulus of matrix, respectively, and Γ_i and Γ_f correspond to the fracture toughness of the interface and fibres.

With regard to the as-received material studied in the present work,

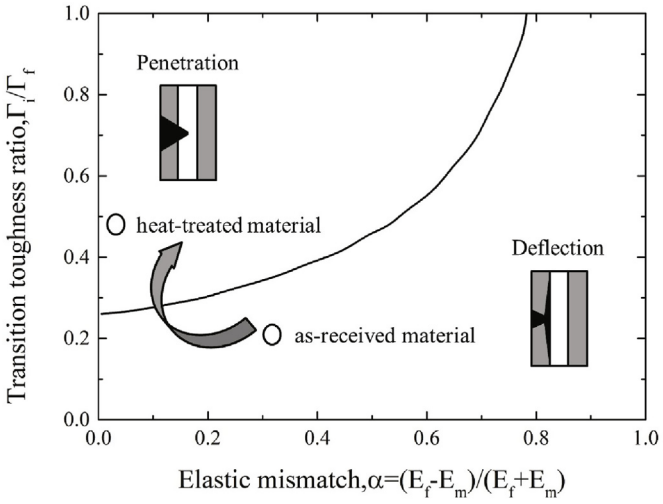

Fig. 8. Relation of crack-propagation modes and material parameters.

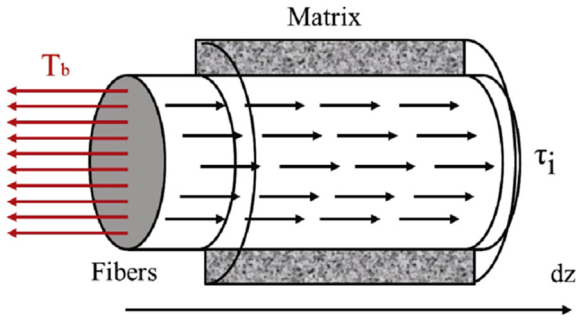

Fig. 9. Schematic diagram of broken fibres.

as there is no fibre coating at the interface and the fibres are sufficiently strong, the ratio Γ_i/Γ_f is very small and the initial value is located below the curve plotted in Fig. 8. Then, according to Table 1, the elastic mismatch parameter $\alpha \approx 0.3$. Thus, the propagation of matrix cracks in the as-received material is deflected at the interface.

However, as mentioned above, after heat treatment, on account of matrix densification, the matrix stiffness increases gradually with increasing thermal-exposure duration. The fibre stiffness does not change significantly during heat treatment [9], and therefore the value of the elastic mismatch parameter $\alpha = (E_f - E_m)/(E_f + E_m)$ is reduced after thermal exposure. Then, fibre bridging establishes a direct connection between the fibre and matrix and induces an enhancement of the interface, increases the value of Γ_i/Γ_f during heat treatment. Therefore, the position of the material in Fig. 8 moves upward and leftward, indicating that the propagation mode of matrix cracks in the composite is transformed from deflection at the interface to penetration into the

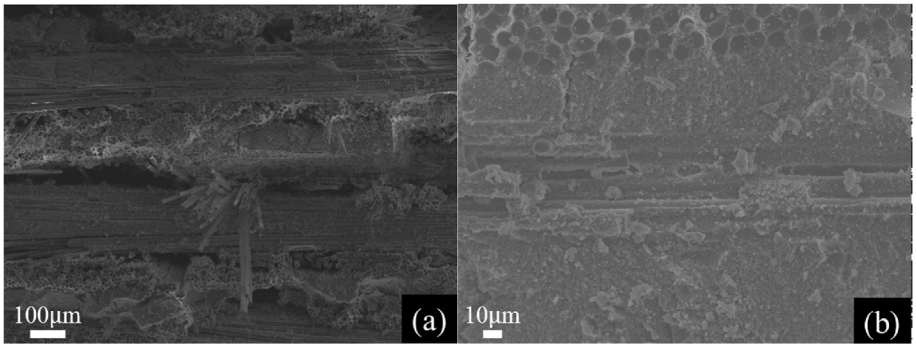

Fig. 7. Fracture surfaces for (a) an as-received tensile specimen, and (b) a specimen after 500 h of thermal exposure.

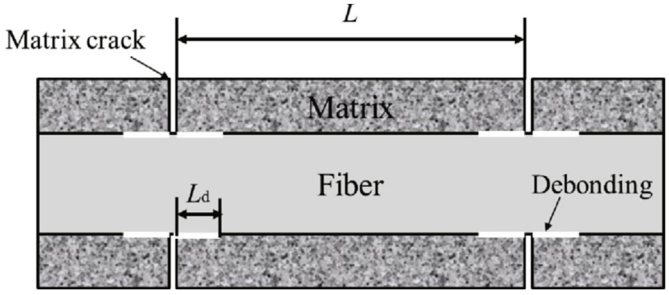

Fig. 10. Mesoscopic diagram of the composite.

Table 3
Material parameters in the mesoscopic model [22].

Material parameter	as-received	100 h	200 h	500 h
σ_c(MPa)	2810	1860	1780	1760
ω	0.09	0.09	0.09	0.09
m	3.3	3.4	3.2	3.3

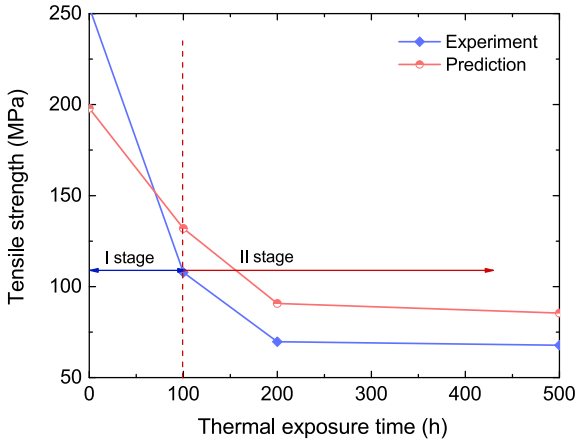

Fig. 11. Theoretical and experimental strengths of the material for different thermal-exposure durations.

fibre. This transition is exhibited in Fig. 8.

As thermal exposure results in the variation of matrix crack propagation mode, in the meantime, with increasing of heat treatment these two factors including variations of fiber and matrix's mechanical properties and matrix crack propagation mode will have significant influence on the strength of the material. A meso-scale mechanical model was adopted to discuss the effects of varying the fibre and interface on the tensile strength of the material.

According to Yang [23], the state of a 2D woven composite can be simplified to the following configuration in Fig. 10:where L is the spacing between matrix cracks for a given applied stress level σ, and L_d is the interfacial debonding length. The present study neglects the tensile residual stress induced by the mismatch between the fibre and matrix thermal expansion coefficients. Based on the theories of Curtin [24], L is defined as

$$L = \frac{r_f K \sigma_f}{2\tau_i} \tag{5}$$

where K is the stress concentration coefficient in the debonding region, calculated from the fibre and matrix properties [23]:

$$K = 1 + \frac{(1 - V_f)E_m}{V_f E_f} \tag{6}$$

and where τ_i is the interfacial shear stress, and r_f is the average fibre radius.

The failure probability distribution for a single fibre is considered to be described by a two-parameter Weibull model:

$$P(T) = 1 - \exp\left[1 - \left(\frac{T}{\sigma_c}\right)^m\right] \tag{7}$$

where T represents the peak stress carried by intact fibres (determined in the matrix crack plane), m is the fibre Weibull modulus (set to 4 in the present work), and σ_c is the characteristic fibre strength with the gauge length δ_c (considered to be twice the debonding length at the current stress level). According to Ref. [25], σ_c and δ_c can be related to the gauge length of the test specimen l_0, which can be expressed as:

$$\sigma_c = \left(\frac{l_0 \sigma_0^m \tau_i}{r_f}\right)^{\frac{1}{m+1}}, \ \delta_c = \left(\frac{\sigma_0 r_f l_0^{\frac{1}{m}}}{\tau_i}\right)^{\frac{m}{m+1}} \tag{8}$$

where σ_0 is the characteristic fibre strength with gauge length l_0.

With increasing load, the bearing capacity of the matrix decreases gradually until the volume fraction of matrix cracks reaches a saturation point [23], denoted η. Then, a further increase in load becomes born entirely by fibres until the fibre stress reaches a critical value, prompting the destructive failure of the composite. Based on the global load sharing assumption, the equilibrium equation for a fibre bundle in the state of ultimate failure, in the presence of debonding, can be written

$$\frac{\sigma}{\omega} = T(1 - P(T)) + \overline{T}_b P(T) \tag{9}$$

where $\overline{T}_b$ represents the stress carried by broken fibres.

According to experimental data [8,22], when the thermal-exposure duration exceeds 100 h, the microstructure and mechanical properties of Nextel™610 fibres become almost independent of the thermal-exposure time. Thus, the heat treatment process can be divided into two stages. In the first stage, the fibre strength decreases owing to grain-size coarsening of the fibres and interface, as a result of fibre bridging. In the second stage, the fibre microstructure tends to be stable and variations in the strength of the material are mainly caused by transition in the matrix-crack propagation mode during tensile loading. Based on these assumptions, the strength of the material, subjected to different heat-treatment times, can be analyzed by the following methods.

4.2.1. *Strength model for the first stage of heat treatment (t<100 h)*

When the heat-treatment time lies within the range for the first stage, In order to calculate the average stress $\overline{T}_b$ in broken fibres, the equilibrium equation for broken fibres can be expressed as:

$$\pi r_f^2 T_b(z) = 2\pi r_f \tau_i dz \tag{10}$$

As the stress in the fracture plane of the broken fibres equals zero, and the stress in the bonded region carried by the broken fibres equals T, the boundary condition of the equation is given by

$$T_b(0) = 0, \ T_b(l_f) = T \tag{11}$$

where 0 represents the location of the fibre fracture plane and l_f is obtained by

$$l_f = \frac{r_f T}{2\tau_i} \tag{12}$$

Then, in the interval [0, l_f], the probability of fibre breakage is considered to be expressed by the distribution [26].

$$F(z) = \frac{1}{P(T) l_f}\left(\frac{T}{\sigma_c}\right)^m (exp)\left[-\frac{z}{l_f}\left(\frac{T}{\sigma_c}\right)^m\right] \tag{13}$$

Hence, according to statistical theory, the average stress in the broken fibres can be calculated as

$$\bar{T}_b = \int_0^{l_f} \left(\int_0^{l_f} T_b(z)dz/z \right) F(l)dl = T\left[\left(\frac{\sigma_c}{T} \right)^m - \frac{1 - P(T)}{P(T)} \right] \tag{14}$$

As the average stress in fibre is determined, substituting Eq. (14) into Eq. (9) yields the applied stress σ as a function of T:

$$\frac{\sigma}{\omega} = T\left(\frac{\sigma_c}{T} \right)^m P(T) \tag{15}$$

The theoretical strength for the material in the first stage can be determined from Eq. (15) by finding the maximum of σ versus T.

4.2.2. Strength model for the second stage of heat treatment

In the second stage, when matrix cracks propagate in the other mode that penetrate the adjacent fibre, it is thought that fibres break in the plane of the matrix cracks. Under this circumstance, the pull-out stress T_b can be neglected and σ versus T in the fibre is expressed as

$$\frac{\sigma}{\omega} = T[1 - P(T)] \tag{16}$$

The corresponding predicted strength can also be obtained using Eq. (16).

4.2.3. Predicted strength of the material for different thermal-exposure durations

The material parameters are listed in Table .3.

Based on the data in Table 3, the material strengths resulting from different thermal-exposure times are predicted by Eqs. (15) and (16). The predictions are compared with experimental results in Fig. 11.

Notably, according to Fig. 11, the predicted strength of the as-received material is smaller than the experimental value, whereas the opposite is true under other conditions. This may result from the coexistence of different matrix-crack propagation modes in the real systems and from the weakening of the degradation of the strength of fibres in-situ by the interface enhancement. In general, the strength model accurately predicts the failure stress of the material after thermal exposure.

From the above analysis, it can be concluded that variations in the tensile strength of the composite originate from two main causes: firstly, the transformation of the failure mechanism induced by matrix densification and interface enhancement; and secondly, the degradation of fibre properties induced by an increase in fibre grain size, in agreement with observations and experimental results.

5. Conclusion

The present study investigated the microstructure and the on-axis tensile properties of oxide/oxide ceramic matrix composites. Measurements of the microstructure and mechanical properties indicate that long-term thermal exposure will cause changes in the microstructure of the material and further induce variations of the macroscopic mechanical properties of the material. The monotonic tensile experiments of as-received and heat-treated materials indicate that thermal exposure significantly influences the on-axis strength of the composite, with little impact on the elastic modulus. The variation in the matrix porosity plays an important role in determining the stiffness. Because of matrix densification and interface enhancement induced by fibre bridging during heat treatment, the matrix-crack propagation mode in the composite changes from deflection at the interface to penetration into the neighbouring fibre. Then, the fibre strength is degraded by grain coarsening. Acting simultaneously, these two factors cause a degradation of the composite strength. By considering the coupling effects of variations in different material properties, the proposed analytical method describes the brittleness and strength degradation of the material after thermal exposure.

Declaration of competing interest

The authors declare that they have no known competing financial interests or personal relationships that could have appeared to influence the work reported in this paper.

Acknowledgement

The present work was supported by the Strategic Priority Research Program of the Chinese Academy of Sciences (Grant No. XDA17030100).

References

[1] W. Yi, C. Haifei, L. Haitao, W. Jun, Microstructure and room temperature mechanical properties of mullite fibers after heat-treatment at elevated temperatures, Mater. Sci. Eng., A 578 (2013) 287–293.
[2] Y. Zhengmao, L. Hui, A continuum damage mechanics model for 2-D woven oxide/oxide ceramic matrix composites under cyclic thermal shocks, Ceram. Int. 46 (5) (2019) 6029–6037.
[3] SM Almeida Renato, Eduardo L. Bergmüller, Lührs Hanna, Michael Wendschuh, Bernd Clauß, Kamen Tushtev, Kurosch Rezwan, Thermal exposure effects on the long-term behavior of a mullite fiber at high temperature, J. Am. Ceram. Soc. 100 (9) (2017) 4101–4109.
[4] Y. Zhengmao, L. Hui, A continuum fatigue damage model for the cyclic thermal shocked ceramic-matrix composites, Int. J. Fatig. 134 (2020) 105507, https://doi.org/10.1016/j.ijfatigue.2020.105507.
[5] Y. Zhengmao, L.I.U. Hui, An elastic-plastic constitutive model for thermal shocked oxide/oxide ceramic-matrix composites, Int. J. Mech. Sci. 175 (2020) 105528, https://doi.org/10.1016/j.ijmecsci.2020.105528.
[6] Martin Schmücker, Peter Mechnich, Improving the microstructural stability of nextel 610 alumina fibers embedded in a porous alumina matrix, J. Am. Ceram. Soc. 93 (7) (2010) 1888–1890.
[7] Martin Schmücker, Ferdinand Flucht, Peter Mechnich, Degradation of oxide fibers by thermal overload and environmental effects, Mater. Sci. Eng., A 557 (2012) 10–16.
[8] Randall S. Hay, Geoff E. Fair, Travis Tidball, Fiber strength after grain growth in nextel™610 alumina fiber, J. Am. Ceram. Soc. 98 (6) (2015) 1907–1914.
[9] Eike Vokmann, Marcelo D. Barros, Kamen Tushtev, E. Walter, C. Pritzkow, Dietmar Koch, Jürgen Göring, Christian Wilhelmi, Georg Grathwohl, Kurosch Rezwan, Influence of the matrix composition and the processing conditions on the grain size evolution of nextel 610 fibers in ceramic matrix composites after heat treatment, Adv. Eng. Mater. 17 (5) (2015) 610–614.
[10] E. Volkmann, L. Lima Evangelista, K. Tushtev, D. Koch, C. Wilhelmi, K. Rezwan, Oxidation-induced microstructural changes of a polymer-derived nextel™ 610 ceramic composite and impact on the mechanical performance, J. Mater. Sci. 49 (2) (Jan 2014) 710–719.
[11] L. Hui, Y. Zhengmao, Y. Huang, A novel elastoplastic constitutive model for woven oxide/oxide ceramic matrix composites with anisotropic hardening, Compos. Struct. 229 (2019) 111420.
[12] SM Almeida Renato, Eduardo L. Bergmüller, Bruno GF. Eggert, Kamen Tushtev, Thomas Schumacher, Lührs Hanna, Bernd Clauß, Georg Grathwohl, Kurosch Rezwan, Thermal exposure effects on the strength and microstructure of a novel mullite fiber, J. Am. Ceram. Soc. 99 (5) (2016) 1709–1716.
[13] M.-L. Antti, E. Lara-Curzio, R. Warren, Thermal degradation of an oxide fibre (nextel 720)/aluminosilicate composite, J. Eur. Ceram. Soc. 24 (3) (2004) 565–578.
[14] Y. Zhengmao, Y. Junjie, Investigation of long-term thermal aging-induced damage in oxide/oxide ceramic matrix composites, J. Eur. Ceram. Soc. 40 (4) (2019) 1549–1556.
[15] B. Moser, A. Rossoll, L. Weber, O. Beffort, A. Mortensen, Nextel 610 alumina fibre reinforced aluminium: influence of matrix and process on flow stress, Compos. Appl. Sci. Manuf. 32 (8) (2001) 1067–1075.
[16] B. Moser, A. Rossoll, L. Weber, O. Beffort, A. Mortensen, Damage evolution of nextel 610tm alumina fibre reinforced aluminium, Acta Mater. 52 (3) (2004) 573–581.
[17] Y. Zhengmao, L. Hui, Y. Huang, Micro-porosity as damage indicator for characterizing cyclic thermal shock-induced anisotropic damage in oxide/oxide ceramic matrix composites, Eng. Fract. Mech. 220 (2019) 106669.
[18] David C.C. Lam, Fred F. Lange, Anthony G. Evans, Mechanical properties of partially dense alumina produced from powder compacts, J. Am. Ceram. Soc. 77 (8) (1994) 2113–2117.
[19] Ming-Yuan He, John W. Hutchinson, Crack deflection at an interface between dissimilar elastic materials, Int. J. Solid Struct. 25 (9) (1989) 1053–1067.
[20] F.W. Zok, C.G. Levi, Mechanical properties of porous-matrix ceramic composites, Adv. Eng. Mater. 3 (12) (2001) 15–23.
[21] Jon Binner, Matt Porter, Ben Baker, Ji Zou, Vinothini Venkatachalam, Virtudes Rubio Diaz, Andrea D'Angio, Prabhu Ramanujam, Tailin Zhang, T.S.R.C. Murthy, Selection, processing, properties and applications of ultra-high temperature ceramic matrix composites, uhtcmcs–a review, Int. Mater. Rev. (2019) 1–56.
[22] J.A. Celemín, J.Y. Pastor, J. LLorca, M. Elices, A. Martín, After thermal exposure at 1200 c, Fract. Mech. Ceram.: Fatig. Compos. High Temp. Behav. 12 (319) (2012).

[23] C.-P. Yang, L. Zhang, B. Wang, T. Huang, G.-Q. Jiao, Tensile behavior of 2D-C/SiC composites at elevated temperatures: experiment and modeling, J. Eur. Ceram. Soc. 37 (4) (2017) 1281–1290.
[24] WA. Curtin, Stochastic Damage Evolution and Failure in Fiber-Reinforced Composites, Adv. Appl. Mech. 36 (1999) 164–253.
[25] A. William, Curtin. Theory of mechanical properties of ceramic-matrix composites, J. Am. Ceram. Soc. 74 (11) (1991) 2837–2845.
[26] S.L. Phoenix, R. Raj, Overview no. 100 scalings in fracture probabilities for a brittle matrix fiber composite, Acta Metall. Mater. 40 (11) (1992) 2813–2828.